Optimal bounds, bounded optimality

Böhm, Udo

Appendix A

Appendix to Chapter 3: 'On the Relationship Between Reward Rate and Dynamic Decision Criteria'

In our theoretical analysis we argued that the shape of the optimal DDC mainly depends on whether sampling costs increase or decrease over time, and that monotonic transformations of the sampling costs should not affect the general shape of the optimal DDC. One prominent example of such transformations is prospect theory which proposes that human decision-making is not governed by the objective losses and wins associated with different decisions, but rather by a non-linear transformation of these quantities, the utility function (Kahneman & Tversky, 1979; Tversky & Kahneman, 1992).

The non-linear utility function is governed by two parameters:

$$u_k(t) = \begin{cases} X(t)^A & \text{if } X(t) \geq 0 \\ -w \cdot |X(t)|^A & \text{if } X(t) < 0, \end{cases} \tag{A.1}$$

where $A \in [0, 1]$ is the shape parameter, and $w \in [0, 5]$ is the loss aversion parameter. The effect of the two parameters on the utility function is illustrated in Figure A.1. As can be seen in the left panel, the A parameter determines the shape of the utility function. For values of A close to 1, the function is nearly linear whilst for values close to 0 it approximates a step function. The right panel shows the effect of the w parameter, which determines the degree to which losses are given higher weight than wins. For values of w close to 1, wins and losses are weighted equally, whilst values close to 0 mean that losses are neglected and values close to 5 mean that losses are overweighted relative to wins.

Figure A.2 shows the optimal decision criterion for the increasing costs condition (left column) and the decreasing costs condition (right column) for different parameterisations of the utility function. As can be seen, although the utility function influences the height of the optimal criterion, it does not change the shape of the criterion. The shape parameter A seems to merely shift the criterion downwards for smaller values of A (compare first and second row of plots). However,

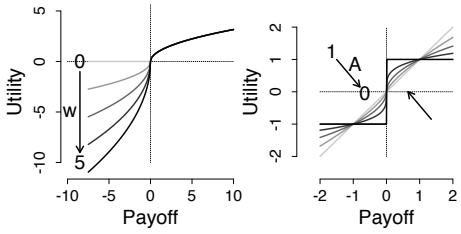

Figure A.1: Effect of the shape (A) and loss aversion parameter (w) on the prospect utility function.

for very small values of A (not shown in the Figure), the optimal decision criterion is flat at 0.5, which means that the optimal decision strategy is to guess immediately, rather than wait for any sensory information. The effect of the loss aversion parameter w is opposite to that of A. Lower values of w shift the decision criterion up whereas lower values shift the criterion down (compare second to fourth row of plots).

These results can be easily explained in light of the utility function. For values of the shape parameter A close to 1, the utility function is nearly linear and the impact of changes in A is largest on large absolute payoffs. Such changes therefore most strongly impact the perceived differences between wins for correct decisions and losses for incorrect decisions, rapidly equalising the perceived values. Consequently, the decision maker stands to gain less from a correct decision and to lose less for an incorrect decision, and should therefore become increasingly willing to risk an incorrect decision due to a low decision criterion, which is reflect by a lower decision criterion. However, for smaller values of the shape parameter, changes in A also affect small absolute payoffs. Therefore, such changes in A increasingly equalise the perceived sampling costs at different points in time and make the perceived sampling costs more similar to the wins and losses for correct and incorrect decisions. Because changes in sampling costs are the driving force behind different shapes of the decision criterion, equalising the perceived sampling costs across time yields a flat optimal criterion. Moreover, because sampling costs are perceived to be numerically equal to wins and losses (for $A = 0$ the utility function returns only the values 1 and $-w$), waiting for even one time step incurs costs that exceed the potential wins for a correct decision, which means that the optimal strategy is to guess immediately.

The loss aversion parameter w determines the perception of negative payoffs, with smaller values of w corresponding to lower weights for negative payoffs. Therefore, small values of w result in small perceived absolute sampling costs, which makes the decision to wait for an additional time step before committing to a decision relatively cheaper and results in a higher decision criterion. However, small values of w do not nullify differences in sampling costs across time to the degree that smaller values of A, thus leaving the shape of the decision criterion intact.

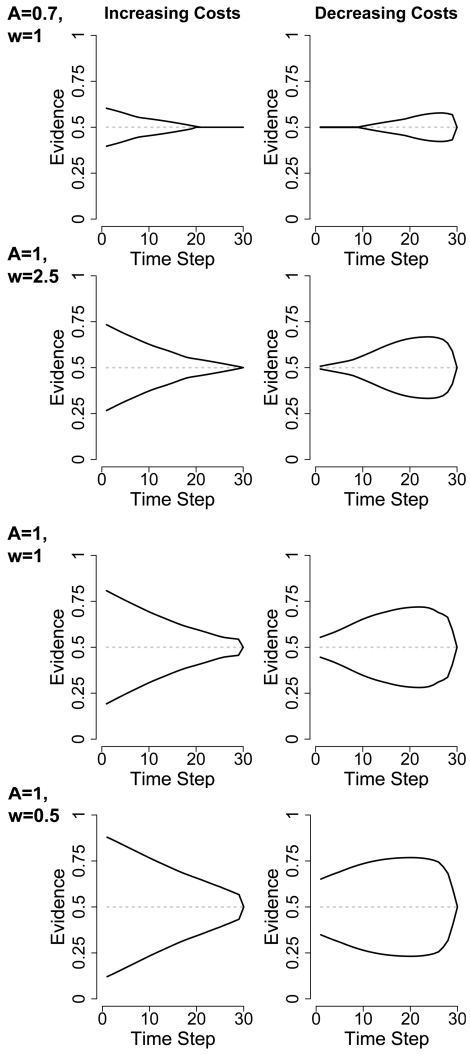

Figure A.2: Optimal bounds for different parameterisations of the prospect utility function.

Appendix B

Appendix to Chapter 4: 'Trial-by-Trial Fluctuations in CNV Amplitude Reflect Anticipatory Adjustment of Response Caution'

Single-trial drift rate by itself is not a better predictor of CNV amplitude than single-trial response caution but contains additional information about CNV amplitude beyond that conveyed by single-trial response caution. We tested whether single-trial drift rate predicts CNV amplitude with the DR × Cond (drift rate) Model (Table B.1), which contained a fixed and a random effect for experimental condition as well as fixed and random effects of single-trial drift rate and the interaction between drift rate and experimental condition. The RC x Cond Model was superior to the DR × Cond Model (ΔAIC = 22; a chi-square test could not be computed because both models had the same number of degrees of freedom), meaning that single-trial drift rate by itself was not as good a predictor of CNV amplitude as single-trial response caution. We investigated further whether single-trial drift rate explains additional variance in CNV amplitude beyond response caution. The RC + DR Model included the same predictors as the RC × Cond Model and additional fixed and random effects for drift rate and drift rate by experimental condition. A formal comparison with the RC × Cond Model showed that the RC + DR Model accounted better for CNV amplitude (ΔAIC = 6; $\chi^2(13) = 35.37$, $p = .002$).

The finding that single-trial drift rate correlates with CNV amplitude in addition to single-trial response caution is critical with respect to the conceptual underpinnings of the single-trial Linear Ballistic Accumulator (STLBA) model. The Linear Ballistic Accumulator (LBA) model decomposes response time and accuracy data into a number of underlying decision processes such as response caution, drift rate, and non-decision time that describe the shape of a participant's response time distribution (S. D. Brown & Heathcote, 2008). The STLBA model then aims to obtain estimates of single-trial response caution and drift rate from the para-

Table B.1: Model parameters for linear mixed effects models of the relationship between drift rate and CNV amplitude.

	DR×Cond Model		DR+Cond Model	
AIC	26860		26832	
	$\hat{\beta}$ (SE)	t-value	$\hat{\beta}$ (SE)	t-value
Intercept	5.665 (2.132)	2.658	0.769 (2.491)	0.309
Condition	-0.491 (2.212)	-0.222	4.743 (3.026)	1.567
DR	8.911 (3.592)	2.481	9.190 (3.254)	2.824
DR×Cond	-5.543 (4.043)	-1.371	-5.738 (4.474)	-1.282
RC			0.024 (0.008)	2.969
RC×Cond			-0.025 (0.010)	-2.511

meters estimated by the LBA model (Ho et al., 2012; Van Maanen et al., 2011). Ideally, these estimates should be independent, which means that a physiological measure of response caution should only be correlated with the model estimates of response caution but not drift rate. Our finding that CNV amplitude correlates with single-trial drift rate implies that either CNV amplitude reflects a mixture of response caution and drift rate or that the STLBA model does not completely separate response caution and drift rate.

Two findings make us confident that the CNV amplitude mostly reflects fluctuations in response caution, rather than drift rate. Firstly, our statistical analysis based on the single-trial parameter estimates showed that response caution is a better predictor of CNV amplitude than drift rate. Secondly, if the CNV amplitude would mostly reflect fluctuations in drift rate, large increases in CNV amplitude should be associated with small increases in response time for short response times whilst small increases in CNV amplitude should be associated with large increases in response time for long response times. Drift rate is the slope of the ballistic trajectory of the accumulated evidence towards the decision boundary (see Figure 4.2). Short response times are caused by a very high drift rate, that is, a very steep slope. At such a steep slope, numerically big changes in drift rate lead to relatively small changes in the point at which the trajectory of the accumulated evidence intersects the decision bound, leading to only minor changes in response time. Long response times, on the other hand, are caused by a low drift rate, that is, very shallow slope of the evidence trajectory. Under these circumstances, numerically small changes in drift rate cause considerable shifts in the point at which the trajectory intersects the decision boundary, giving rise to large changes in response time.

Our exploratory GAMs analysis of the raw response time data showed that small increases in CNV amplitude are associated with large increases in response time for short response times whilst, according to the above reasoning, if the CNV amplitude would reflect drift rate, large changes in CNV amplitude should be associated with small changes in response times for fast responses. Similarly, we found that larger increases in CNV amplitude are associated with small increases in response time for longer response times whilst the above reasoning implies that the opposite should be the case if CNV amplitude reflected drift rate. This finding

Table B.2: Model parameters for linear mixed effects of the relationship between response time and CNV amplitude at FCz for different time windows.

Time Window	-0.10 to -0.20s					
	Baseline Model		RT Model		RT×Cond Model	
AIC	28566		28550		28529	
	$\hat{\beta}$ (SE)	t-value	$\hat{\beta}$ (SE)	t-value	$\hat{\beta}$ (SE)	t-value
Intercept	10.021 (1.405)	7.134	11.504 (2.036)	5.650	15.288 (2.864)	5.338
Cond	-3.157 (0.836)	-3.774	-1.929 (0.839)	-2.300	-8.052 (2.411)	-3.340
RT			-0.003 (0.004)	-2.054	-0.010 (0.003)	-3.186
RT×Cond					0.001 (0.003)	3.114
Time Window	-0.55 to -0.45s					
AIC	28051		28050		28039	
	$\hat{\beta}$ (SE)	t-value	$\hat{\beta}$ (SE)	t-value	$\hat{\beta}$ (SE)	t-value
Intercept	8.176 (1.167)	7.008	8.746 (1.602)	5.460	11.761 (2.242)	5.245
Cond	-2.992 (0.708)	-4.225	-2.481 (0.698)	-3.552	-7.392 (1.983)	-3.72
RT			-0.001 (0.001)	-1.065	-0.007 (0.003)	-2.708
RT×Cond					0.008 (0.003)	3.010
Time Window	-1.05 to -0.95s					
AIC	27426		27423		27422	
	$\hat{\beta}$ (SE)	t-value	$\hat{\beta}$ (SE)	t-value	$\hat{\beta}$ (SE)	t-value
Intercept	4.859 (0.763)	6.367	5.343 (1.201)	4.451	6.49 (1.780)	3.655
Cond	-1.207 (0.475)	-2.543	-0.864 (0.695)	-1.243	-2.879 (1.819)	-1.582
RT			-0.001 (0.001)	-0.710	-0.003 (0.002)	-1.351
RT×Cond					0.003 (0.002)	1.338
Time Window	-1.55 to -1.45s					
AIC	26690		26692		26699	
	$\hat{\beta}$ (SE)	t-value	$\hat{\beta}$ (SE)	t-value	$\hat{\beta}$ (SE)	t-value
Intercept	4.152 (0.681)	6.100	5.022 (0.928)	5.409	5.029 (1.160)	4.336
Cond	-1.035 (0.490)	-2.112	-0.380 (0.558)	-0.680	-0.459 (1.516)	-0.303
RT			-0.002 (0.001)	-1.654	-0.002 (0.001)	-1.079
RT×Cond					< 0.001 (0.002)	0.055

Note. Experimental condition is dummy-coded as SP=0 and AC=1.

implies that CNV amplitude does not reflect fluctuations in drift rate but rather in response caution.

Table B.3: Model parameters for linear mixed effects of the relationship between response time and CNV amplitude at Cz for different time windows.

Time Window	-0.10 to -0.20s					
	Baseline Model		RT Model		RT×Cond Model	
AIC	28938		28914		28902	
	$\hat{\beta}$ (SE)	t-value	$\hat{\beta}$ (SE)	t-value	$\hat{\beta}$ (SE)	t-value
Intercept	9.251 (1.541)	6.002	11.171 (2.368)	4.717	14.692 (2.977)	4.935
Cond	-2.920 (0.723)	-4.039	-1.539 (0.850)	-1.810	-7.466 (2.120)	-3.522
RT			-0.004 (0.002)	-2.144	-0.010 (0.003)	-3.328
RT×Cond					0.009 (0.003)	3.258
Time Window	-0.55 to -0.45s					
AIC	28235		28226		28218	
	$\hat{\beta}$ (SE)	t-value	$\hat{\beta}$ (SE)	t-value	$\hat{\beta}$ (SE)	t-value
Intercept	7.492 (1.295)	5.786	8.289 (1.932)	4.291	11.437 (2.438)	4.691
Cond	-2.827 (0.653)	-4.332	-2.253 (0.717)	-3.141	-7.602 (1.737)	-4.377
RT			-0.002 (0.001)	-1.176	-0.007 (0.002)	-3.009
RT×Cond					0.008 (0.002)	3.543
Time Window	-1.05 to -0.95s					
AIC	27475		27464		27468	
	$\hat{\beta}$ (SE)	t-value	$\hat{\beta}$ (SE)	t-value	$\hat{\beta}$ (SE)	t-value
Intercept	4.240 (1.044)	4.061	4.864 (1.666)	2.921	6.040 (1.935)	3.121
Cond	-1.005 (0.447)	-2.251	-0.648 (0.708)	-0.916	-2.652 (1.464)	-1.812
RT			-0.001 (0.001)	-0.744	-0.003 (0.002)	-1.416
RT×Cond					0.003 (0.002)	1.443
Time Window	-1.55 to -1.45s					
AIC	26552		26547		26555	
	$\hat{\beta}$ (SE)	t-value	$\hat{\beta}$ (SE)	t-value	$\hat{\beta}$ (SE)	t-value
Intercept	3.066 (0.871)	3.520	3.910 (1.251)	3.126	3.877 (1.285)	3.018
Cond	-0.943 (0.469)	-2.011	-0.330 (0.502)	-0.657	-0.322 (1.417)	-0.227
RT			-0.002 (0.001)	-1.377	-0.001 (0.001)	-0.998
RT×Cond					> -0.001 (0.002)	-0.003

Note. Experimental condition is dummy-coded as SP=0 and AC=1.

Table B.4: Model parameters for linear mixed effects of the relationship between response time and CNV amplitude at the electrode with maximum AC-SP difference per participant for different time windows.

Time Window	-0.10 to -0.20s					
	Baseline Model		RT Model		RT×Cond Model	
AIC	29681		29677		29673	
	$\hat{\beta}$ (SE)	t-value	$\hat{\beta}$ (SE)	t-value	$\hat{\beta}$ (SE)	t-value
Intercept	8.353 (0.567)	14.741	6.047 (0.885)	6.832	2.539 (1.317)	1.928
Cond	2.857 (0.680)	4.206	1.217 (0.802)	1.518	7.294 (2.022)	3.607
RT			0.004 (0.001)	3.360	0.010 (0.002)	4.995
RT×Cond					-0.009 (0.003)	-3.502
Time Window	-0.55 to -0.45s					
AIC	44320		44318		44322	
	$\hat{\beta}$ (SE)	t-value	$\hat{\beta}$ (SE)	t-value	$\hat{\beta}$ (SE)	t-value
Intercept	6.182 (0.431)	14.353	4.761 (0.817)	5.826	3.318 (1.425)	2.329
Cond	1.181 (5.370)	2.199	0.102 (0.843)	0.121	2.620 (1.568)	1.671
RT			0.002 (0.001)	1.842	0.005 (0.003)	1.871
RT×Cond					-0.004 (0.002)	-1.431
Time Window	-1.05 to -0.95s					
AIC	27869		27876		27879	
	$\hat{\beta}$ (SE)	t-value	$\hat{\beta}$ (SE)	t-value	$\hat{\beta}$ (SE)	t-value
Intercept	4.447 (0.339)	13.136	4.730 (0.588)	8.050	2.841 (0.929)	3.058
Cond	0.305 (0.514)	0.593	0.543 (0.595)	0.914	3.926 (1.396)	2.812
RT			-0.001 (0.001)	-0.590	0.003 (0.002)	1.852
RT×Cond					-0.005 (0.002)	-2.645
Time Window	-1.55 to -1.45s					
AIC	26767		26775		42629	
	$\hat{\beta}$ (SE)	t-value	$\hat{\beta}$ (SE)	t-value	$\hat{\beta}$ (SE)	t-value
Intercept	2.335 (0.308)	7.590	2.622 (0.507)	5.179	1.647 (0.928)	1.776
Cond	0.316 (0.403)	0.783	0.530 (0.503)	1.054	2.149 (1.244)	1.727
RT			-0.001(0.001)	-0.706	0.001 (0.001)	0.825
RT×Cond					-0.002 (0.002)	-1.412

Note. Experimental condition is dummy-coded as SP=0 and AC=1.

Table B.5: Model parameters for linear mixed effects of the relationship between response time and CNV amplitude at the electrode with maximum AC-SP difference per participant for different time windows.

Time Window	-0.10 to -0.20s					
	Baseline Model		RT Model		RT×Cond Model	
AIC	26862		26862		26838	
	$\hat{\beta}$ (SE)	t-value	$\hat{\beta}$ (SE)	t-value	$\hat{\beta}$ (SE)	t-value
Intercept	9.942 (1.400)	7.100	8.740 (1.294)	6.753	5.160 (1.167)	4.422
Cond	-3.079 (0.853)	-3.609	-3.615 (0.965)	-3.746	1.858 (1.576)	1.179
RT			0.006 (0.003)	1.851	0.024 (0.007)	3.469
RT×Cond					-0.025 (0.008)	-3.037
Time Window	-0.55 to -0.45s					
AIC	26379		26386		26368	
	$\hat{\beta}$ (SE)	t-value	$\hat{\beta}$ (SE)	t-value	$\hat{\beta}$ (SE)	t-value
Intercept	8.142 (1.157)	7.040	8.139 (1.179)	6.904	5.282 (1.520)	3.475
Cond	-2.870 (0.682)	-4.206	-2.926 (0.692)	-4.228	1.067 (1.55)	0.687
RT			¡0.001 (0.003)	0.049	0.015 (0.006)	2.354
RT×Cond					-0.019 (0.008)	-2.530
Time Window	-1.05 to -0.95s					
AIC	10920		10926		10921	
	$\hat{\beta}$ (SE)	t-value	$\hat{\beta}$ (SE)	t-value	$\hat{\beta}$ (SE)	t-value
Intercept	4.807 (0.740)	6.499	4.829 (0.842)	5.733	3.828 (1.323)	2.894
Cond	-1.179 (0.485)	-2.430	-1.193 (0.536)	-2.227	-0.062 (1.627)	-0.038
RT			> -0.001 (0.003)	-0.076	0.005 (0.006)	0.885
RT×Cond					-0.006 (0.007)	-0.827
Time Window	-1.55 to -1.45s					
AIC	10195		10200		10209	
	$\hat{\beta}$ (SE)	t-value	$\hat{\beta}$ (SE)	t-value	$\hat{\beta}$ (SE)	t-value
Intercept	0.425 (0.069)	6.123	0.350 (0.077)	4.567	0.309 (0.094)	3.297
Cond	-0.108 (0.052)	-2.054	-0.137 (0.057)	-2.413	-0.077 (0.110)	-0.703
RT			< 0.001	1.748	0.001 (< 0.001)	1.593
RT×Cond					> -0.001 (< 0.001)	-0.634

Note. Experimental condition is dummy-coded as SP=0 and AC=1.

Table B.6: Model parameters for linear mixed effects of the relationship between response caution and CNV amplitude at Cz for different time windows.

Time Window	-0.10 to -0.20s					
	Baseline Model		RT Model		RT×Cond Model	
AIC	27200		27194		27182	
	$\hat{\beta}$ (SE)	t-value	$\hat{\beta}$ (SE)	t-value	$\hat{\beta}$ (SE)	t-value
Intercept	9.116 (1.476)	6.177	7.598 (1.287)	5.906	4.326(1.288)	3.359
Cond	-2.770 (0.755)	-3.667	-3.335 (0.822)	-4.056	1.410 (1.558)	0.905
RT			0.007 (0.003)	2.047	0.023(0.006)	3.643
RT×Cond					-0.021 (0.007)	-2.925
Time Window	-0.55 to -0.45s					
AIC	26550		26552		26547	
	$\hat{\beta}$ (SE)	t-value	$\hat{\beta}$ (SE)	t-value	$\hat{\beta}$ (SE)	t-value
Intercept	7.407 (1.249)	5.931	7.251 (1.122)	6.462	4.715 (1.149)	4.104
Cond	2.658 (0.623)	-4.269	-2.817 (0.652)	-4.319	0.659 (1.397)	0.472
RT			< 0.001 (0.003)	0.286	0.013 (0.005)	2.433
RT×Cond					-0.015 (0.006)	-2.473
Time Window	-1.05 to -0.95s					
AIC	39853		39852		39861	
	$\hat{\beta}$ (SE)	t-value	$\hat{\beta}$ (SE)	t-value	$\hat{\beta}$ (SE)	t-value
Intercept	3.140 (0.867)	3.622	2.259 (0.786)	2.872	2.280 (1.107)	2.059
Cond	-0.956 (0.486)	-1.968	-1.336 (0.573)	-2.331	-1.234 (1.216)	-1.014
RT			0.004 (0.002)	1.931	0.004 (0.003)	1.186
RT×Cond					-0.001 (0.042)	-0.025
Time Window	-1.55 to -1.45s					
AIC	10195		10200		10209	
	$\hat{\beta}$ (SE)	t-value	$\hat{\beta}$ (SE)	t-value	$\hat{\beta}$ (SE)	t-value
Intercept	0.425 (0.069)	6.123	0.350 (0.077)	4.567	0.309 (0.094)	3.297
Cond	-0.108 (0.052)	-2.054	-0.137 (0.057)	-2.413	-0.077 (0.110)	-0.703
RT			< 0.001 (< 0.001)	1.748	0.001 (< 0.001)	1.593
RT×Cond					> -0.001 (< 0.001)	-0.634

Note. Experimental condition is dummy-coded as SP=0 and AC=1.

Appendix C

Appendix to Chapter 5: 'Using Bayesian Regression to Test Hypotheses About Relationships Between Parameters and Covariates in Cognitive Models'

In this appendix we provide the results of our simulation study for all four parameters of the PVL-Delta model. Figure C.1 gives the log-Bayes factors for all PVL-Delta parameters from our simulations with uncorrelated covariates. Dark grey dots show the Bayes factors obtained in the regression analysis, light grey dots show the Bayes factors obtained in the median-split analysis. Recall that our simulated data were generated so that the first covariate would be positively correlated with the A parameter and the second covariate would be negatively correlated with the w parameter. The correlations between A and the second covariate, and between w and the first covariate were set to 0 and the relationships between the remaining model parameters and the covariates were set to the values estimated from Steingroever et al.'s (in press) data, and were negligible. As described in the main text, the Bayes factors from the regression analysis showed strong evidence for an effect of the first covariate on the A parameter (dark grey dots, left column in the top row) whereas the median-split analysis provided much weaker evidence for such an effect (light grey dots, left column in the top row). Similarly, the regression analysis strongly supported an effect of the second covariate on the w parameter (dark grey dots, second column in the bottom row), whereas the median-split analysis provided weaker evidence for such an effect (light grey dots, second column in the bottom row). For the null-effects of the first covariate on the w parameter (second column, top row) and of the second covariate on the A parameter (left column, bottom panel), both analyses performed similarly without any appreciable differences in Bayes factors. Finally, both analyses provided only weak support if any for an effect the covariates on the a and c parameters and

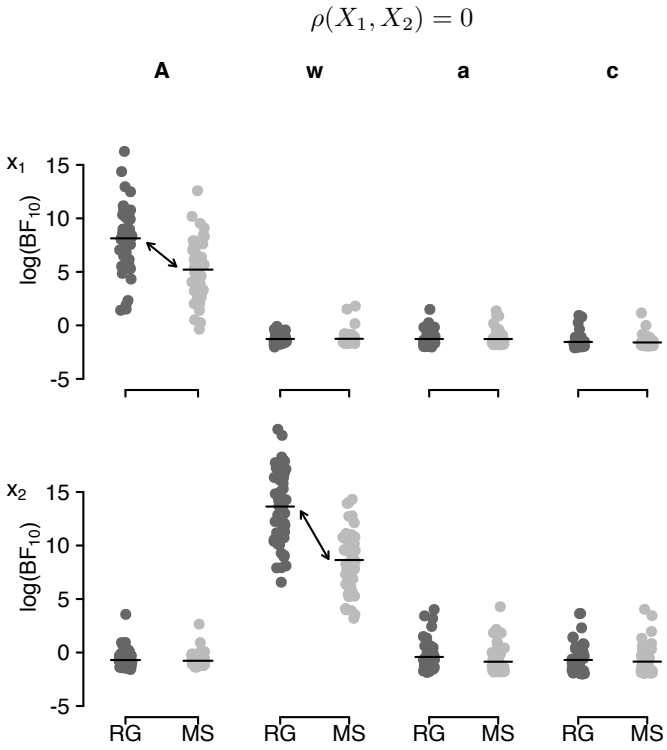

Figure C.1: Bayes factors from 50 simulated data sets for the regression and median-split analysis with uncorrelated covariates. Data points show the log-Bayes factors for the alternative hypothesis ($\log(\mathrm{BF}_{10})$) obtained in the regression (RG, dark grey dots) and median-split (MS, light grey dots) analysis for the PVL-Delta model's A and w parameters (columns) and two covariates (rows). Lines indicate the mean log-BF. Arrows highlight underestimation of Bayes factors in the median-split analysis. Data points are jittered along the x-axis for improved visibility.

there were no sizable differences in Bayes factors.

Figure C.2 gives the log-Bayes factors for all PVL-Delta parameters from our simulations with correlated covariates. As described in the main text, the Bayes factors obtained from the regression analysis again showed stronger evidence for an effect of the first covariate on the A parameter (dark grey dots, left column in the top row) than the median-split analysis (light grey dots, left column in the top row). Similarly, the regression analysis provided stronger support for an effect of the second covariate on the w parameter (dark grey dots, second column in the bottom row), than the median-split analysis (light grey dots, second column in the bottom row). However, unlike in the case of uncorrelated covariates, in the case of correlated covariates the median-split analysis now suggested spurious effects of the first covariate on the w parameter (second column, top row) and of the second covariate on the A parameter (left column, bottom row). Finally, the regression

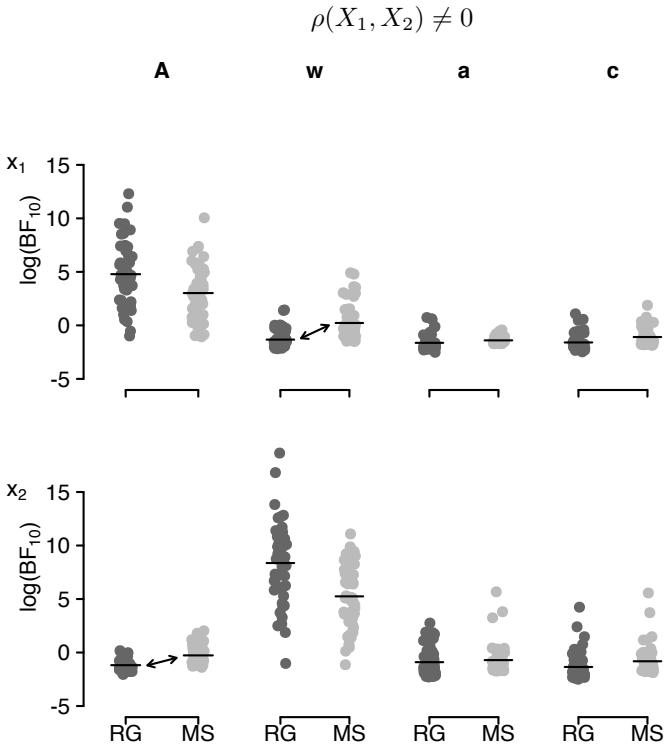

Figure C.2: Bayes factors from 50 simulated data sets for the regression and median-split analysis with correlated covariates. Data points show the log-Bayes factors for the alternative hypothesis ($\log(\mathrm{BF}_{10})$) obtained in the regression (RG, dark grey dots) and median-split (MS, light grey dots) analysis for the PVL-Delta model's A and w parameters (columns) and two covariates (rows). Lines indicate the mean log-BF. Arrows highlight overestimation of Bayes factors in the median-split analysis. Data points are jittered along the x-axis for improved visibility.

as well as the median-split analysis did not provide strong evidence for any effects of the covariates on the a and c parameters, and there were no clear differences in Bayes factors visible between the two analyses.

Taken together, these results illustrate that, in the case of uncorrelated covariates, a median-split analysis tends to understate the evidence for existent effects. In the case of correlated covariates, a median-split analysis also understates the evidence for existent effects but in addition suggests spurious effects of covariates on model parameters that are in fact unrelated. Furthermore, our results show that in cases where model parameters do not have any appreciable relationships with any of the covariates, as was the case for the a and c parameters, regression and median-split analyses perform similarly and there are no appreciable biases associated with a dichotomisation-based analysis.

Figure C.3 shows the posterior means of the standardised effect sizes estimated

in the regression analysis (RG, left panels in each subplot) and the posterior means of the standardised effect sizes estimated in the median-split analysis (MS, right panels in each subplot). The left subplot shows results for the case of uncorrelated covariates, the right subplot shows the results for the case of correlated covariates. The top row shows the results for the first covariate, the bottom row for the second covariate. The results corroborate the results from the Bayes factors. In the case of uncorrelated covariates (left subplot), the estimated effects in both models are largest for effects that we created to be non-zero (i.e., the effect of the first covariate on A and the effect of the second covariate on w, leftmost column of the panels in the top row and second-from-left column of the panels in the bottom row, respectively). Moreover, both models correctly estimate the direction of the effect of the first covariate on the A parameter to be positive (leftmost column of the panels in the top row), and the direction of the effect of the second covariate on w to be negative (second-from-left column of the panels in the bottom row). Both models also correctly estimate the effects of the first and second covariate on a and c to be close to 0 (second-from-right and rightmost columns of each panel).

In the case of correlated covariates (right subplot), both analyses again correctly estimate the size and direction of the strong effects of the first covariate on the A parameter (leftmost column of the panels in the top row) and of the second covariate on the w parameter (second-from-left column of the panels in the bottom row). However, while the regression analysis correctly estimates the relationships between the first covariate and the w parameter (left panel, second-from-left column in the top row) and between second covariate and the A parameter (left panel, leftmost column in the bottom row) to be approximately 0, the median-split analysis suggests a weakly negative association between the first covariate and w (right panel, second-from-left column in the top row) and between the second covariate and A (right panel, leftmost column in the bottom row). Finally, both models correctly estimate the effects of the covariates on the a and c parameters to be close to 0.

These results align well with the results for the Bayes factors. In the case of uncorrelated covariates, the regression analysis as well as the median-split analysis correctly indicate the direction and size of the relationships between covariates and model parameters. However, in the case of correlated covariates, the median-split analysis tends to suggest spurious relationships between covariates and model parameters. The direction of these spurious effects is equal to the direction of the true effects. This suggests a spill-over from one covariate to the other that arises from the fact that the median-split analysis ignores the correlation between covariates, whereas the regression analysis partials out correlations between covariates.

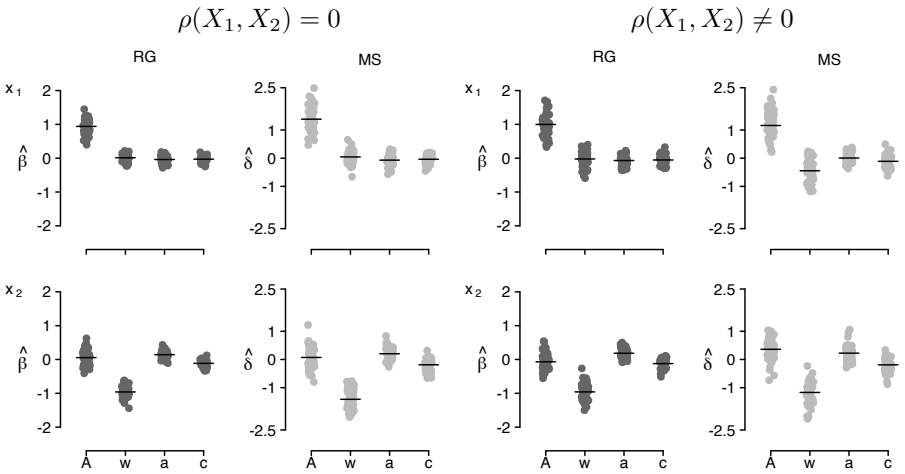

Figure C.3: Mean posterior estimates from 50 simulated data sets of effects for the regression and median-split analysis for uncorrelated (left subplot) and correlated (right subplot) covariates. Data points show the estimated standardised effect sizes ($\hat{\beta}$) from the regression analysis (RG; left panels in each subplot, dark grey dots) and the estimated standardised effect size ($\hat{\delta}$) from the median-split analysis (MS; right panels in each subplot, light grey dots) for the four PVL-Delta parameters. The top row shows the results for the first covariate, the bottom row for the second covariate. Black lines indicate the mean across simulations. Data points are jittered along the x-axis for improved visibility.